

Isoelectronic Oxygen Trap in ZnTe

J. L. MERZ

Bell Telephone Laboratories, Murray Hill, New Jersey

(Received 18 July 1968)

An optical transition at 1.986 eV in ZnTe has earlier been attributed to the radiative recombination of an electron-hole pair bound at an oxygen atom substituting isoelectronically for Te. In this paper the results of isotopic substitution and Zeeman experiments are offered to prove the correctness of this identification. Crystals of ZnTe grown in the presence of ZnO¹⁸ exhibit an isotope shift of the B ($J=2$) line 0.45 ± 0.05 meV to higher energies. At 1.7°K, this is observed both for the no-phonon line and its LO phonon replicas. Zeeman analysis of the $J=2$ quintet shows that the impurity center has the cubic symmetry of the ZnTe zinc-blende lattice, and is therefore a point defect. The dominant character of the B -line emission is found to be forced electric dipole, produced by the magnetic field mixing of B ($J=2$) and A ($J=1$) states.

I. INTRODUCTION

AN interesting optical spectrum was observed in ZnTe by Dietz, Thomas and Hopfield¹ in 1962. This spectrum is reproduced in Fig. 1. A no-phonon line is observed at 1.986 eV both in absorption and in emission. The photoluminescence spectrum consists of a series of longitudinal optical (LO) phonon replicas of this no-phonon line, separated by 26 meV, with several broad acoustic phonon wings between each. The entire vibronic spectrum is mirrored in absorption on the high-energy side of the no-phonon line. This absorption band tends to give the crystals a red appearance so the name "red center" was applied to it. Through a series of doping and annealing experiments, it was suspected that this spectrum resulted from the radiative recombination of an electron-hole pair (exciton) bound to a substitutional oxygen atom at a tellurium site.^{2,3} The spectrum appeared when crystals were grown in quartz vessels, and its strength increased when ZnO was added to the starting material. Annealing in zinc vapor followed by rapid quenching also increased the spectrum. Additional evidence for the presence of oxygen has since been reported.^{4,5} However, all this evidence is admittedly circumstantial and hence inconclusive. In this paper, conclusive evidence for the above-suggested model is offered. The role played by oxygen is confirmed by the results of isotopic substitution, while a Zeeman analysis of the no-phonon line indicates that the center is a point defect. Since it is unlikely that oxygen would form bonds in an interstitial position and produce the simple optical spectrum to be described, the model of an exciton bound to a substitutional oxygen atom is felt to be correct.

The importance of this identification lies in the fact that oxygen and tellurium are isoelectronic, and until recently it was unexpected that such a substitution should form a bound state in the forbidden band of a

semiconductor. In the large majority of cases, an alloy or mixed system is formed. The only other carefully documented cases of these "isoelectronic traps" are GaP:N,^{6,7} GaP:Bi,⁸ and CdS:Te.^{9,10} The mechanism by which such a substitution could bind an exciton is not fully understood; however, it is believed that the center could bind an electron or hole by a strong, short-range interaction when a large electronegativity difference exists between the impurity and the host atom it replaces. The resulting charged center could then bind an oppositely-charged particle through the long-range Coulomb interaction, producing a center which behaves like an "isoelectronic" donor or acceptor.² Although a detailed theoretical understanding of this mechanism has not yet been forthcoming, important progress has been made by Faulkner and Hopfield.^{11,12} One aspect of great practical significance is the fact that, unlike the case of an exciton bound to a neutral donor or acceptor, only two particles are involved in an isoelectronic trap. Therefore, nonradiative Auger recombination via a third particle does not occur, and since these traps can be several hundred meV below the conduction band, highly efficient photoluminescence is observed in some cases even at room temperature.¹³

For a cubic crystal such as ZnTe, the excited state of an isoelectronic trap is a doublet resulting from the coupling of a $j_1 = \frac{3}{2}$ hole with a $j_2 = \frac{1}{2}$ electron. The doublet splitting is 1.6 meV for the case of ZnTe:O. The upper level has total angular momentum $J=1$; transitions from this level to the $J=0$ ground state are allowed electric dipole, and a strong line (referred to as the A line) is seen in photoluminescence at most temperatures. This is the 1.986-eV no-phonon line seen in Fig. 1. The

⁶ D. G. Thomas, J. J. Hopfield, and C. J. Frosch, *Phys. Rev. Letters* **15**, 857 (1965).

⁷ D. G. Thomas and J. J. Hopfield, *Phys. Rev.* **150**, 680 (1966).

⁸ F. A. Trumbore, M. Gershenson, and D. G. Thomas, *Appl. Phys. Letters* **9**, 4 (1966).

⁹ A. C. Aten, J. H. Haanstra, and H. deVries, *Philips Res. Rept.* **20**, 395 (1965).

¹⁰ J. D. Cuthbert and D. G. Thomas, *J. Appl. Phys.* **39**, 1573 (1968).

¹¹ R. A. Faulkner, *Phys. Rev.* **175**, 991 (1968).

¹² R. A. Faulkner and J. J. Hopfield, in *Proceedings of the International Conference on Localized Excitations in Solids*, edited by R. F. Wallis (Plenum Press, Inc., New York 1968), p. 218.

¹³ T. C. Madden, J. L. Merz, G. L. Miller, and D. G. Thomas, *IEEE Trans. Nucl. Sci.* **NS-15**, 47 (1968).

¹ R. E. Dietz, D. G. Thomas, and J. J. Hopfield, *Phys. Rev. Letters* **8**, 391 (1962).

² J. J. Hopfield, D. G. Thomas, and R. T. Lynch, *Phys. Rev. Letters* **17**, 312 (1966).

³ D. G. Thomas, *J. Phys. Soc. Japan Suppl.* **21**, 265 (1966).

⁴ D. I. Kennedy and M. J. Russ, *J. Appl. Phys.* **38**, 4387 (1967).

⁵ G. W. Iseler and A. J. Strauss, *Bull. Am. Phys. Soc.* **13**, 404 (1968).

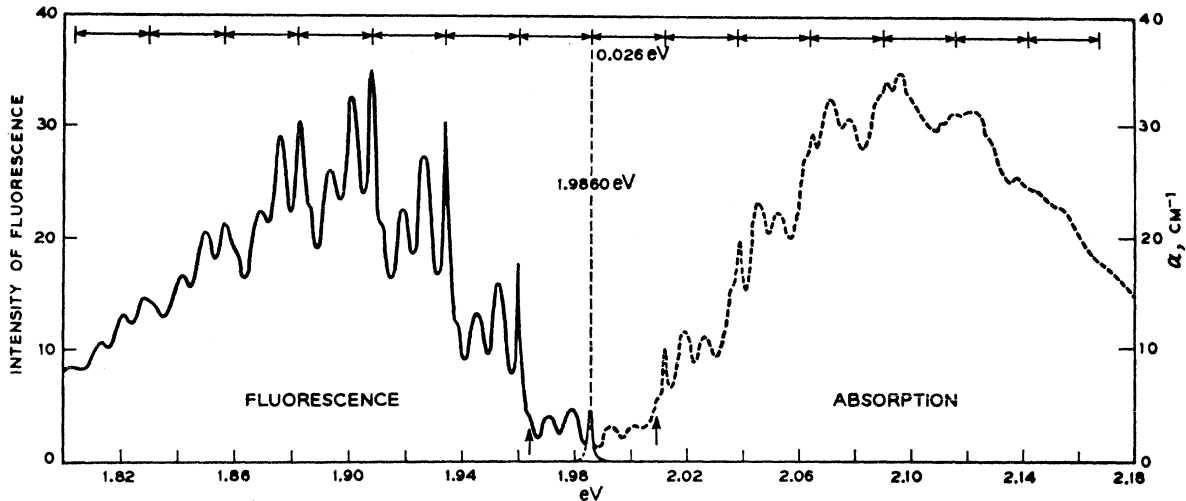


FIG. 1. The fluorescence and absorption of the red center in ZnTe at 20°K. The no-phonon A line occurs at 1.9860 eV, and sharp LO phonon replicas, separated by 26 meV, are mirrored about this central line. The broad peaks within each repeated interval are transverse and longitudinal acoustic phonons. The arrows indicate transverse optical phonons (from Ref. 1).

lower level of the doublet has $J=2$ and is therefore a forbidden transition. However, as the temperature is reduced below 4.2°K, the upper level is thermally depopulated and a new emission line (called the B line) is observed from the $J=2$ state, with a correspondingly longer lifetime. Lifetime measurements as a function of temperature have been made for all of the known isoelectronic traps,^{10,14} and the results are in agreement with the above description. In different materials these lifetimes vary between 9 and 900 nsec for the A line (τ_A) and between 0.3 and 4 μ sec for the B line (τ_B). This spread in decay times depends on the nature of the transition in different materials (direct or indirect band gap), whereas the value of the ratio τ_B/τ_A for a given material has been associated with the type of center involved (isoelectronic "donor" or "acceptor").

II. EXPERIMENTAL

A. Crystal Growth

In order to dope ZnTe with appreciable concentrations of oxygen, most of the crystals used for these experiments were grown by a "mineralization" technique¹⁵ in a sealed quartz tube, usually with 0.1% ZnO added to the charge. In this procedure, the ampoule containing the charge is placed in a flat temperature zone in the furnace, minimizing vapor transport of material from one end of the ampoule to the other. Instead crystals begin to grow or "mineralize" out of the charge; single crystals 4 to 6 mm on a side were obtained, with shiny faces suitable for photoluminescence experiments. Often these crystals were triangular platelets.

The starting material was synthesized from 99.999% pure Zn and Te obtained from the United Mineral and

Chemical Corp. The synthesized ZnTe was further purified, along with the ZnO dopant if desired, by heating to 1090°C for 60 to 80 min in an open quartz tube with a 1-liter/min flow of argon gas. During this process, small (1 or 2 mm) crystallites grew on the walls of the open tube downstream from the charge. After cooling to room temperature and removing the crystallites, the remaining charge was sealed with argon gas to give 1 atm pressure at the growth temperature, replaced in the furnace and heated to \sim 1080°C for 140 h to mineralize larger crystals from the charge. The O^{18} isotope was added in the form of ZnO^{18} , produced by reacting Zn with O^{18} gas (99.6% O^{18} enrichment) obtained from Oak Ridge National Laboratory.

It was found experimentally that the oxygen luminescence was much brighter from the small crystallites produced in the purification procedure than from the mineralized plates. These latter could be made more efficient by etching, possibly because of the acid dissolution of a thin Zn layer which tends to form on the surface of crystals during mineralization.

One crystal selected for much of the Zeeman work reported here (crystal 417627AA) was grown in a similar but slightly different way. The charge was placed in a tube closed by sliding one tightly fitting tube within another. A vacuum seal was therefore not produced, and a flow of argon gas was maintained over the double-tube assembly. This procedure yielded several large single crystals which were easily oriented for Zeeman experiments, but it was not satisfactory for isotope-doping experiments because the system was not vacuum sealed.

B. Optical Experiments

Photoluminescence spectra were measured photographically with a 2-m Bausch & Lomb spectrograph, having a dispersion of 2 Å/mm. An argon ion laser was

¹⁴ J. D. Cuthbert and D. G. Thomas, Phys. Rev. **154**, 763 (1967).

¹⁵ R. T. Lynch, D. G. Thomas, and R. E. Dietz, J. Appl. Phys. **34**, 706 (1963).

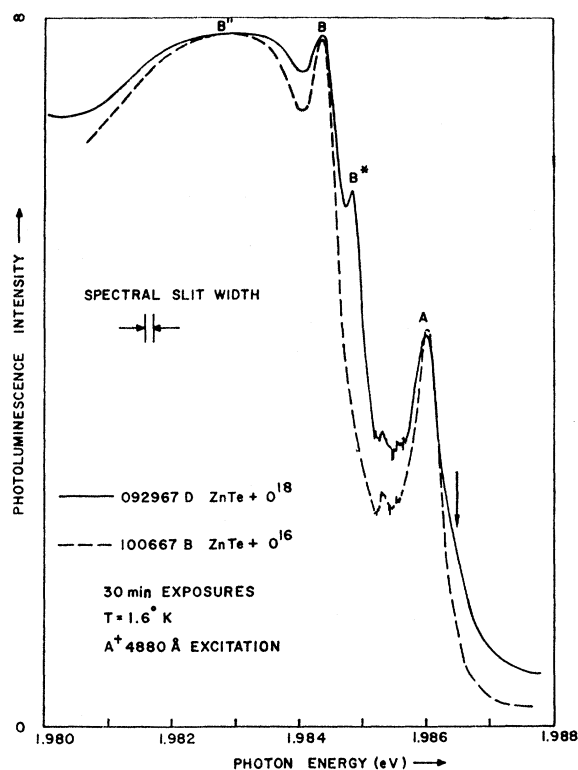


FIG. 2. Photoluminescence intensity of two oxygen-doped samples of ZnTe, one of which contains the isotope O^{18} . Between the A ($J=1$) and B ($J=2$) no-phonon lines, an isotope-shifted B line (denoted by B^*) appears for the sample doped with O^{18} . The isotope shift of the B line is 0.45 ± 0.05 meV. The band at B'' is a phonon-assisted virtual transition. The arrow indicates the region of broadening of the A line due to its weak, unresolved isotope line.

used as the excitation source. Crystals could be cooled to pumped He temperature in a glass cryostat mounted between the poles of a Varian magnet producing fields up to 31 000 G.

The normal Zeeman configuration was used for the magnetic field experiments: $\mathbf{k}' \perp \mathbf{H}$, where \mathbf{k}' is the direction of observation. The incident laser beam made an angle of approximately 20° with \mathbf{k}' . Orientations were generally chosen so that \mathbf{E} , \mathbf{H} , and \mathbf{k}' were all parallel to major crystallographic directions in the ZnTe zinc blende lattice. However, in cases where the normal to the crystal surface made an angle with \mathbf{k}' , then \mathbf{k}' represents the direction of propagation outside the crystal only. The true propagation vector \mathbf{k} inside the crystal is found from Snell's Law.

III. OXYGEN ISOTOPE EXPERIMENT

A. Results

Figure 2 shows the high-resolution spectrum for two crystals, one of which was grown with ZnO^{18} . This is a densitometer recording of a photographic plate in the region near the A and B lines, taken at $1.6^\circ K$. At this temperature the B line is considerably stronger than the

A line. The broader band labelled B'' has been interpreted by Dietz *et al.*¹ as a virtual transition from B to A accompanied by the emission of acoustic phonons; this is of no further interest in the discussion. The only major difference between the spectra is the appearance of a new line (B^*) located 0.45 ± 0.05 meV above the B line, seen only for the crystal grown in the presence of the O^{18} isotope. The B^* line was absent in crystals to which the isotope was not added, but was present in crystals grown either during the purification or mineralization procedures when O^{18} was added. Longitudinal and transverse optical (LO and TO) phonon replicas of the B^* line can be seen, and these replicas also occur 0.45 meV higher in energy than the LO and TO replicas of the B line. No change in these lattice LO or TO phonon energies is observed as a result of isotopic substitution.

B. Discussions of Isotope Results

The line B^* is interpreted to be an isotope shift of the no-phonon B line due to the radiative recombination of an exciton bound at an O^{18} site. By comparing intensities of B and B^* in Fig. 2, it is evident that the concentration of O^{18} is quite low compared to that of the natural O^{16} isotope which is unintentionally present. This is not unexpected, since ZnTe grown by vapor transport in quartz tubes generally contains the oxygen "red center," which can be effectively eliminated only by coating the quartz tubes with pyrolytic graphite.¹⁶ It is therefore speculated that the oxygen is released from the quartz.

An isotope shift of the no-phonon line results when the zero-point vibrations of the ground and excited states of the transition are shifted different amounts by a non-linear electron-phonon interaction. This effect has already been observed for excitons bound to isoelectronic nitrogen and to Cd-O nearest-neighbor pairs in GaP,^{7,17-19} and for no-phonon lines in various donor-acceptor pair emission spectra involving deep states.^{20,21} For the case of an exciton bound to a Cd-O complex in GaP, the O^{18} isotope shift of the no-phonon line was found to be 0.65 meV,¹⁷ comparable in magnitude to that observed here.

The isotope shift of the A line is difficult to observe, because of homogeneous broadening by rapid phonon-assisted transitions to the B state.¹ The full width at half-height of the A line is approximately 1 meV, more than twice the isotope shift measured for the B line. In

¹⁶ D. T. F. Marple and M. Aven, in *Proceedings of the International Conference on II-VI Semiconducting Compounds*, edited by D. G. Thomas (W. A. Benjamin, Inc., New York, 1967), p. 315.

¹⁷ C. H. Henry, P. J. Dean, D. G. Thomas, and J. J. Hopfield, in *Proceedings of the International Conference on Localized Excitations in Solids*, edited by R. F. Wallis (Plenum Press, Inc., New York, 1968), p. 267.

¹⁸ T. N. Morgan, B. Welber, and R. N. Bhargava, *Phys. Rev.* **166**, 751 (1968).

¹⁹ C. H. Henry, P. J. Dean, and J. D. Cuthbert, *Phys. Rev.* **166**, 754 (1968).

²⁰ P. J. Dean, C. H. Henry, and C. J. Frosch, *Phys. Rev.* **168**, 812 (1968).

²¹ P. J. Dean, C. J. Frosch, and C. H. Henry, *J. Appl. Phys.* **39**, 5631 (1968).

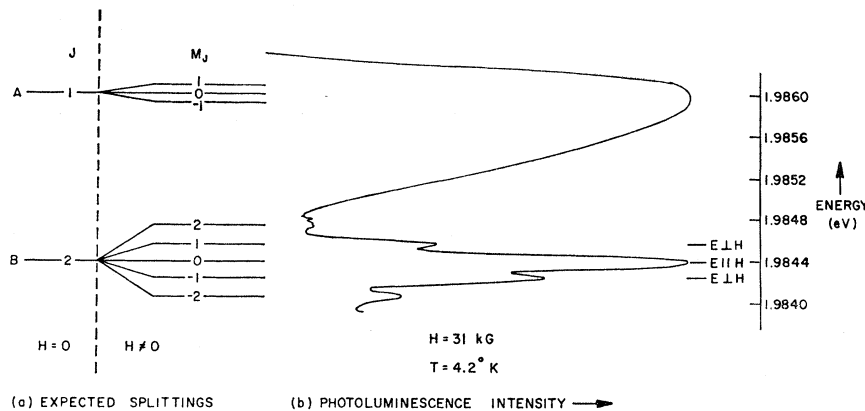


FIG. 3. Zeeman splittings of the A and B no-phonon lines. (a) shows the expected Zeeman pattern, and (b) is a typical densitometer trace for sample 417627AA. The A -line splitting cannot be resolved because of the smaller splitting and lifetime broadening of this state. The B -line quintet is clearly observed, with the $M_J=0, \pm 1$ components polarized as shown.

Fig. 2 long exposures and wide slits (200μ) were used in order to clearly observe the presence or absence of the B^* isotope line; the sharp B and B^* lines therefore appear broad. (The large width of the A line compared to that of the B line is better seen in the Zeeman spectrum of Fig. 3, photographed under more favorable conditions for line-width determinations.) The intensity of the A line at 1.6°K is also much weaker than it appears relative to B in Fig. 2 because of the nonlinearity of the photographic emulsion. For these reasons an isotope-shifted A line is very difficult to observe, although there is evidence of broadening on the high-energy side of the A line in the vicinity of the expected isotope line (arrow in Fig. 2).

The isotope shift of the R lines of chromium in ruby and MgO has been treated by Imbusch *et al.*²²⁻²⁴ They measured the temperature-dependent frequency shift of these lines, and used this value to calculate the temperature-independent shift (and hence the isotope shift) on the basis of the Debye model. However, this approach cannot be used in the present case for several reasons. The temperature-dependent shift of the A and B lines in ZnTe is difficult to measure because of thermalization between them and because of thermal liberation of the weakly bound hole. Interpretation of this data is further complicated by the fact that the band gap of a semiconductor shifts with temperature, and unlike the case of chromium in ruby or MgO , a bound exciton in a semiconductor is strongly influenced by such lattice effects.

In most cases where an isotope shift has been observed, the lack of mirror symmetry between absorption and emission implies a large value for the nonlinear electron-phonon interaction responsible for the shift. In the case of ZnTe , the linear interaction term is much stronger, as is evident from the mirror symmetry in Fig. 1. However, this does not prevent the observation of an isotope shift; McCumber has found from sym-

metry considerations alone that the linear term does not contribute to the strain-induced frequency shift.²⁵ Dean *et al.*²¹ have suggested that the isotope shift of the no-phonon line is associated with a large central cell component of the binding energy of the exciton, and in the case of an isoelectronic trap such as oxygen in ZnTe , the binding of the tightly bound particle is entirely a central cell effect.^{11,12}

Despite these obvious difficulties in calculating the magnitude of the observed isotope shift, such a shift has been clearly identified for the incorporation of O^{18} into ZnTe , and proves that oxygen is indeed responsible for the spectrum of Fig. 1. It remains to show that this center is a substitutional point defect, and therefore must result from the replacement of a lattice Te ion by a single oxygen impurity.

IV. MAGNETIC AND CRYSTAL-FIELD EFFECTS

A study of the Zeeman splittings of bound exciton lines yields a great deal of information about the degeneracies of the lines and the orientation of the trapping center in the lattice. A typical Zeeman spectrum for oxygen-doped ZnTe is shown in Fig. 3, taken at 4.2°K in a field $H=31\,000 \text{ G}$. Figure 3(a) shows the splitting pattern expected for an exciton bound to an isoelectronic trap in a cubic semiconductor like ZnTe ; the A state ($J=1$) splits into a triplet and the B state ($J=2$) into a quintet. The quintet is clearly observed but the splitting of the A state is not for two reasons: (1) the splitting of the A line depends on the difference of the hole and electron g values rather than the sum (as is the case for the B line),²⁶ and (2) the lifetime broadening of the A line is appreciable. Of the five components of the B line, the central component ($M_J=0$) is polarized parallel with the magnetic field, while the $M_J=\pm 1$ components are polarized perpendicular to the field. (The outer components with $M_J=\pm 2$ are usually weak and will be discussed in Sec. IV C) This is the polarization pattern expected for an electric dipole

²² G. F. Imbusch, W. M. Yen, A. L. Schawlow, G. E. Devlin, and J. P. Remeika, *Phys. Rev.* **136**, A481 (1964).

²³ G. F. Imbusch, W. M. Yen, A. L. Schawlow, D. E. McCumber, and M. D. Sturge, *Phys. Rev.* **133**, A1029 (1964).

²⁴ D. E. McCumber and M. D. Sturge, *J. Appl. Phys.* **34**, 1682 (1963).

²⁵ D. E. McCumber, *J. Math. Phys.* **5**, 221; **5**, 508 (1964).

²⁶ D. G. Thomas, M. Gershenzon, and J. J. Hopfield, *Phys. Rev.* **131**, 2397 (1963).

transition from a state with total angular momentum $J=1$, and could arise by magnetic field mixing of the A and B lines such that the $M_J=1, 0$, and -1 components of A were mixed into the $M_J=1, 0$, and -1 components of B , respectively.

A. Mixing of the A and B Lines

The spin Hamiltonian for a $j_1=\frac{3}{2}$ hole and a $j_2=\frac{1}{2}$ electron bound to an ionized donor has been described by Yafet and Thomas,²⁷ and holds equally well for isoelectronic traps.²⁸

$$\mathcal{H} = \mathcal{H}^{(C)} + \mathcal{H}^{(Z)}, \quad (1)$$

$$\mathcal{H}^{(C)} = -a\mathbf{j}_1 \cdot \mathbf{j}_2 - b(j_{1x}^3 j_{2x} + j_{1y}^3 j_{2y} + j_{1z}^3 j_{2z}), \quad (2a)$$

$$\mathcal{H}^{(Z)} = \mu_B [K\mathbf{j}_1 \cdot \mathbf{H} + L(j_{1x}^3 H_x + j_{1y}^3 H_y + j_{1z}^3 H_z) + g_e \mathbf{j}_2 \cdot \mathbf{H}]. \quad (2b)$$

$\mathcal{H}^{(C)}$ is the crystal-field term, $\mathcal{H}^{(Z)}$ is the Zeeman term, K and L are the g factors of the anisotropic hole, g_e is the electron g factor, and μ_B is the Bohr magneton. The $J=1$ level is unsplit in a cubic crystal field, while the splitting of the $J=2$ level is small; this will be discussed in Sec. IV B. The Zeeman term splits the levels into a triplet and a quintet. If the axis of quantization (z axis) is chosen along the magnetic field direction, Eq. (2b) reduces to

$$\mathcal{H}^{(Z)} = (Kj_{1z} + Lj_{1z}^3 + g_e j_{2z}) \mu_B H. \quad (3)$$

The wave functions for the $J=1$ and $J=2$ states ($|j_1 j_2 J M_J\rangle$) can be expanded in terms of the single-particle wave functions ($|j_1 j_2 m_1 m_2\rangle$) as usual:

$$|j_1 j_2 J M_J\rangle = \sum_{m_1, m_2} |j_1 j_2 m_1 m_2\rangle \times \langle j_1 j_2 m_1 m_2 | j_1 j_2 J M_J \rangle, \quad (4a)$$

or more simply,

$$|J M_J\rangle = \sum_{m_1, m_2} |m_1 m_2\rangle \langle m_1 m_2 | J M_J \rangle, \quad (4b)$$

where the quantities $\langle m_1 m_2 | J M_J \rangle$ are the ordinary Clebsch-Gordan coefficients. The Hamiltonian $\mathcal{H}^{(Z)}$ of Eq. 3 mixes the $J=1$ states into some of the $J=2$ states, and to first order the perturbation yields

$$|2, \pm 2\rangle^{(1)} = |2, \pm 2\rangle^{(0)}, \quad (5a)$$

$$|2, \pm 1\rangle^{(1)} = |2, \pm 1\rangle^{(0)} \pm \epsilon_1 |1, \pm 1\rangle^{(0)}, \quad (5b)$$

$$|2, 0\rangle^{(1)} = |2, 0\rangle^{(0)} + \epsilon_0 |1, 0\rangle^{(0)}, \quad (5c)$$

where

$$\epsilon_1 = \frac{1}{4} \sqrt{3} [K + (13/4)L - g_e] \beta H / E_{1,2}, \quad (6a)$$

$$\epsilon_0 = \frac{1}{2} (K + \frac{1}{4}L - g_e) \beta H / E_{1,2}. \quad (6b)$$

²⁷ Y. Yafet and D. G. Thomas, Phys. Rev. **131**, 2405 (1963).

²⁸ The analysis of the A and B lines in GaP (Ref. 27) assumes that these lines result from the recombination of an exciton bound to an ionized donor. It has since been shown that these lines are associated with the isoelectronic trap nitrogen (Refs. 6 and 7), but the spin-Hamiltonian description of this center remains unaltered.

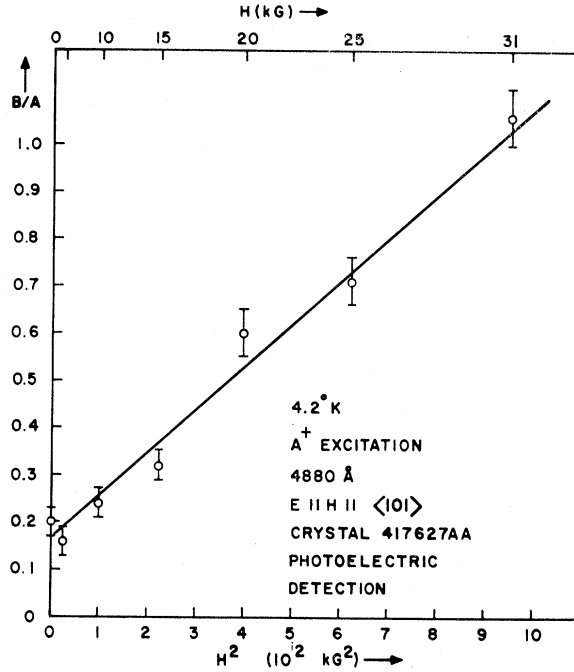


FIG. 4. Ratio of B -line to A -line intensities as a function of the square of the magnetic field. An orientation was chosen where the $M_J=\pm 1$ components were unobservable, to reduce error. The linear relationship of B/A to H^2 indicates that H is mixing the $J=1$ and $J=2$ states. Photoelectric detection was used for accurate intensity measurements.

$|J, M_J\rangle^{(0)}$ and $|J, M_J\rangle^{(1)}$ are the zeroth- and first-order wave functions, respectively, and $E_{1,2}$ is the energy separation between the $J=1$ and $J=2$ states. (Here we have assumed that the difference between the A and B line splittings is negligible compared to $E_{1,2}$.) The mixing of the $J=1$ levels into the $J=2$ levels is therefore linear in the magnetic field strength H , so the intensity of the electric dipole transitions from these levels to the ground state will vary as the square of the field.

To test that this is the case, the intensity ratio B/A was measured as a function of the field from zero to 31 000 G. This was done at 4.2°K using the polarization $\mathbf{E} \parallel \mathbf{H}$, so that the central component of the B line was compared with the intensity at the center of the A line. The results are shown in Fig. 4. A plot of B/A versus H^2 is found to be a straight line to within the accuracy of the experiment. Thus, the assumption made above is felt to be correct: The dominant contribution to the B line in a magnetic field is electric dipole in character resulting from the field mixing of the A and B lines. The nonzero value of B/A at zero field represents the degree of thermalization occurring at 4.2°K along with any residual strain mixing that may be present. (Note that this strain cannot be considerable since the B line is sharp and unsplit in zero field.)

B. Crystal-Field Splitting

The symmetry of the electron and hole wave functions in a cubic crystal field has already been discussed

by Yafet and Thomas;²⁷ the $J=2$ level is split by the crystal-field Hamiltonian [Eq. (2a)] into a doublet whose levels have symmetry Γ_3 and Γ_5 . The $J=1$ level is unsplit. The energies of these levels are given by

$$J=1: E(\Gamma_4) = (5/4)a + (41/16)b, \quad (7a)$$

$$J=2: E(\Gamma_3) = -\frac{3}{4}a - (15/16)b, \quad (7b)$$

$$E(\Gamma_5) = -\frac{3}{4}a - (39/16)b. \quad (7c)$$

The splitting of the $J=2$ level is therefore $\frac{3}{2}b$, with the Γ_5 level lying lowest. The splitting could not be observed directly; in zero magnetic field the $B(J=2)$ line appears to be a singlet with half-width of approximately 0.1 meV.

However, in a magnetic field there is an increased possibility of observing this crystal-field splitting. Examination of the wave functions shows that the central component ($M_J=0$) of the B line is a pure Γ_5 state when the magnetic field is parallel with the crystal $[111]$ axis, while this component is pure Γ_3 for $\mathbf{H} \parallel [100]$. A careful study of the Zeeman data, to be described below, showed that the $M_J=0$ component was consistently lower in energy for $\mathbf{H} \parallel [111]$ than for $\mathbf{H} \parallel [100]$, by approximately 0.03 to 0.05 meV. However, the scatter and uncertainty in this data is of the same order of magnitude, so this determination of the B -line crystal-field splitting is at the limit of detectability. From this it can be concluded that the parameter b in Eqs. (2) and (7) has the value $0 < b \leq 0.04$ meV. Note that these are essentially the same results found for the B line in GaP.²⁶

C. Zeeman Effect

1. Energy Splittings

The Zeeman splitting of the B line was studied for various orientations of the magnetic field, electric field, and direction of propagation relative to major crystallographic directions. The results are summarized in Fig. 5. For the cases where the magnetic field is parallel to the $[100]$, $[111]$, and $[011]$ axes, the crystal was mounted so that it could be rotated about the $[0\bar{1}1]$ axis. Polarizers were used so that the electric vector was either perpendicular to \mathbf{H} (parallel to the $[0\bar{1}1]$ axis), or parallel to \mathbf{H} . The external propagation vector (\mathbf{k}) was corrected as described in Sec. II B to obtain the true propagation vector (\mathbf{k}) inside the crystal; these results are all listed in Fig. 5. The case for $\mathbf{H} \parallel [101]$ is not equivalent to $\mathbf{H} \parallel [011]$; to achieve $\mathbf{H} \parallel [101]$ the crystal was removed from the sample stick and remounted in the desired orientation.

All of these cases were studied in crystal 417627AA. The orientation of this crystal could be determined by inspection of the smooth as-grown faces, and x-ray diffraction photographs were taken to verify that this orientation was correct. Zeeman splitting was also studied in various crystals grown during the purification or mineralization procedures described in Sec. II A. These crystals were generally unoriented, but the mag-

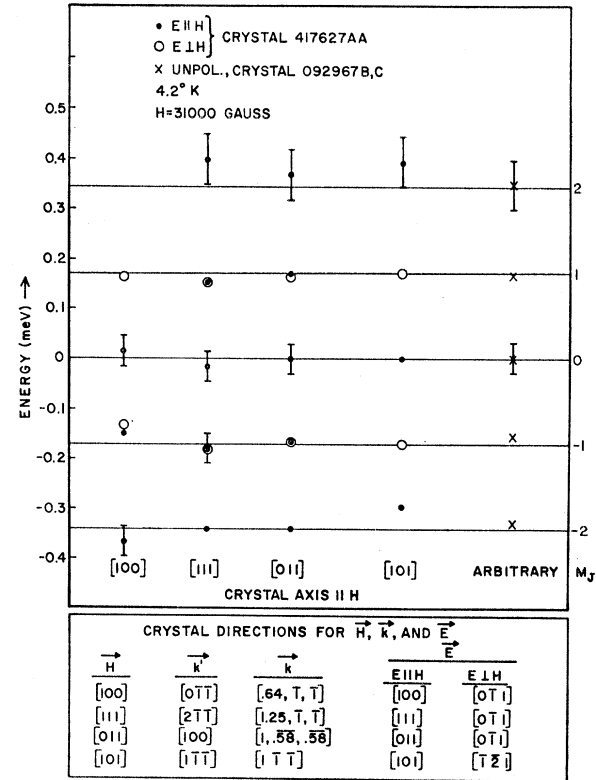


Fig. 5. Zeeman energy-splitting diagram for four different crystallographic directions parallel to the magnetic field. Points are plotted for both $E \parallel H$ and $E \perp H$ polarization. Data for an arbitrary crystal orientation are also given (unpolarized). The table summarizes the directions of \mathbf{E} , \mathbf{H} , \mathbf{k}' (direction of observation), and \mathbf{k} (direction of propagation within the crystal) relative to the crystal axes. The error is larger for the $M_J=2$ line because this transition is weak. The results indicate that the oxygen impurity center is a point defect.

nitude of the splitting and polarization of the components are in close agreement with the results for crystal 417627AA. The results for one of these unoriented crystals are also included in Fig. 5 (listed as arbitrary direction).

The scatter and uncertainty in this data is approximately ± 0.03 meV, indicated by the error bars which have been placed on a few of the points in Fig. 5. Note that the central component for $\mathbf{H} \parallel [100]$ has been displaced about 0.03 meV to higher energy above the $\mathbf{H} \parallel [111]$ central component. This represents the small crystal-field effect discussed above, although the displacement is well within the error bars. The error associated with the highest energy component ($M_J=2$) is greater than for the other Zeeman components because the weak intensity of this line makes it difficult to determine its peak energy in the background noise. (For example, see Fig. 3 for an actual densitometer trace.) The lowest energy component ($M_J=-2$) is much stronger because of thermalization.

The data plotted in Fig. 5 shows that all five components of the B line are seen for each orientation of the crystal in the magnetic field. The energy separation of

adjacent components is approximately constant: 0.17 meV for a field of 31 000 G. A small amount of anisotropy in the energy splitting can also be seen in the figure; this anisotropy results from the anisotropic hole term in Eq. (2b). The important fact emerging from this data is the complete lack of any strong orientation dependence of the Zeeman splitting, indicating that the center responsible for these spectra is a point defect. These results are very similar to those obtained for the *A* and *B* lines in GaP,²⁷ which have recently been shown to result from the isoelectronic substitution of nitrogen for a phosphorus atom.²⁸ The substitution of oxygen for tellurium in ZnTe is a closely analogous situation. If the center was not a point defect, but instead was comprised of a pair of impurity atoms, an impurity and a lattice defect, or some other combination of associated defects, then the center would have a well-defined axis within the crystal. Not only the magnitude of the splitting but also the number of components observed would then differ for the cases where \mathbf{H} is parallel and perpendicular to the axis of the defect. Such a result was found for the case of an exciton bound to a Cd-O nearest-neighbor pair in GaP; this complex has $[111]$ symmetry in the crystal.¹⁹ The Zeeman splitting pattern for this complex showed six lines with the crystal in an arbitrary direction, four lines with $\mathbf{H} \parallel [111]$, three lines with $\mathbf{H} \parallel [011]$, and two lines with $\mathbf{H} \parallel [100]$. Moreover, the crystal-field splitting of the *B* line was unobservably large in this case. These effects are clearly not observed for the case of ZnTe doped with oxygen.

2. Intensities of Zeeman Components

Although the energy splittings of the *B* line were found to be largely independent of crystal orientation, indicating that the center is a point defect, interesting intensity variations were observed for the Zeeman components. Representative results are shown in Fig. 6. These data are presented in the form of bar graphs showing the relative intensities of the five Zeeman components for the four orientations included in Fig. 5 ($\mathbf{E} \parallel \mathbf{H}$ in each case). To obtain this intensity data the photographic emulsion used (type 103a-F) has been calibrated with neutral density filters. Correction has been made for the thermalization occurring at 4.2°K, the temperature of the measurements. The $M_J=0$ central component is always strong with this parallel polarization, and the other components have all been normalized to the strength of this central line.

The error involved in calibrating photographic intensities is large, up to 25% for some of the lines plotted in Fig. 6. However, the figure clearly indicates that the intensities of the $M_J = \pm 2$ lines vary appreciably relative to the $M_J = \pm 1$ lines for different crystal orientations. This suggests that a mechanism such as electric quadrupole transitions may be operative for these outer components, and an attempt was made to explain the intensity patterns with this hypothesis.

The anisotropy of electric quadrupole transitions in

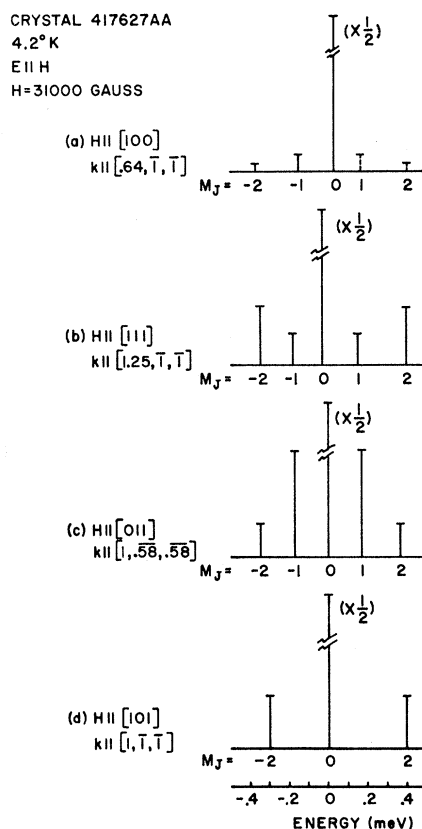


Fig. 6. Bar graph showing approximate relative intensities of Zeeman components for the orientations summarized in Fig. 1. All intensities are normalized to the $M_J=0$ central component, which has been reduced by a factor of $\frac{1}{2}$ in this graph to display the other components. The dotted lines in (a) mean that the $M_J = +1$ and $+2$ components could not be observed in this orientation. Intensities have been corrected for temperature thermalization and photographic response.

Cu_2O has been investigated by Elliott, Gross, and others.²⁹⁻³¹ The treatment of Elliott is applicable to the ZnTe case, with two complications: (1) the crystal field does not split the Γ_3 and Γ_5 wave functions sufficiently, so both symmetries contribute to the five Zeeman components, and (2) the direction of propagation, \mathbf{k} , cannot be expressed as simple integers because of the crystal refraction pointed out earlier. The wave functions for the $J=2$ quintuplet can be written in terms of the five spherical harmonics of order two, three of which transform as the Γ_5 representation of the cubic point group ($\varphi_{xy}, \varphi_{yz}, \varphi_{zx}$), and two transform as Γ_3 ($\varphi_x^2, \varphi_x^2 - y^2$). Then, by choosing the direction of the magnetic field as the axis of quantization for each of the orientations under consideration, the Zeeman component wave functions d_{M_J} can be written as linear combinations of these spherical harmonics, with one adjustable parameter expressing the relative strengths

²⁹ R. J. Elliott, Phys. Rev. 124, 340 (1961).

³⁰ E. F. Gross, B. P. Zakharchenya, and A. I. Sibilev, Fiz. Tverd. Tela 4, 1003 (1962) [English transl: Soviet Phys.—Solid State 4, 739 (1962)].

³¹ V. I. Cherenov and V. S. Galishev, Fiz. Tverd. Tela 3, 1085 (1961) [English transl.: Soviet Phys.—Solid State 3, 790 (1961)].

of the Γ_3 and Γ_5 components. Once these wave functions are obtained, matrix elements can be calculated with the quadrupole Hamiltonian expanded in terms of second-order spherical harmonics according to the method of Elliott. The resulting transition probabilities depend on the direction indices for \mathbf{k} and \mathbf{E} .

The results of these calculations were reasonably consistent with much of the intensity data, at least to the accuracy mentioned above, but there were a few exceptions. Notable among these was case (d) in Fig. 6, where $\mathbf{H} \parallel [101]$ and $\mathbf{k} \parallel [1\bar{1}\bar{1}]$. The theory predicts a nonvanishing intensity for $d_{\pm 1}$, while $d_{\pm 2} = 0$. The opposite is observed experimentally. The failure to observe a theoretically predicted line presents no serious difficulty, since a longer exposure may be needed. However, the observation of a line predicted to vanish indicates that the quadrupole mechanism is not sufficient and that another effect is also being observed. Nor can this anomalous case be explained by a cubic crystal-field mixing of the components of the B line. Equation (2a) is the most general two-particle spin Hamiltonian that can be written for a crystal with T_d symmetry, and this Hamiltonian can only mix the $M_J = \pm 2$ components into each other. Some other effect must be responsible for the nonvanishing of the $M_J = \pm 2$ components, possibly a small amount of strain in the crystal. These intensity experiments must therefore be regarded as somewhat inconclusive.

It has been shown (Sec. IV A) that the predominant effect is the electric dipole transition from the $M_J = 0, \pm 1$ levels resulting from the magnetic field mixing of the A and B lines. The weaker transitions observed from the $M_J = \pm 2, \pm 1$ levels are believed to result from electric quadrupole plus higher-order effects, but systematic quantitative proof of this is lacking.

V. CONCLUSIONS

The role played by oxygen in the photoluminescent spectrum of the "red center" in ZnTe has been confirmed by the observation of an isotope-shifted no-phonon line when the crystals are doped with O^{18} . An analysis of the Zeeman effect for this center shows that it has the symmetry of the zinc blende lattice, and must therefore be a simple point defect. This is supported by the absence of any fine structure in the A and B lines. The possibility that this spectrum results from an oxygen atom in an interstitial position is considered to be extremely remote, for several reasons: (a) Oxygen forms strong tetrahedral bonds, and it is unexpected that it would bond in an interstitial position. (b) Interstitial oxygen would act as a complicated acceptor; it would be fortuitous if the introduction of such an impurity could produce the simple A and B line spectrum resulting from a single electron and hole coupling to the impurity. (c) The magnitude of the crystal-field splitting of the B line would be expected to be much larger if the center were located in an interstitial position. This

accumulation of evidence that the "red center" defect is a substitutional point defect involving oxygen is strong confirmation of the model proposed by Hopfield *et al.*²: The spectrum results from the radiative recombination of an electron-hole pair bound at the oxygen isoelectronic trap. Supporting evidence for the importance of oxygen has been mentioned in the Introduction; however, the isotope experiment reported in this paper proves that the active defect is oxygen and not another defect carried into the crystal along with oxygen.

Recent work has been reported by Tanimizu and Otomo on the thermoluminescence and annealing effects in melt-grown ZnTe.³² They observe a strong enhancement of the red-center luminescence when the crystals are annealed in zinc at 850°C for 60 h, and this enhancement is accompanied by the appearance of a new edge emission line at 2.330 eV. They attribute both these lines to the same center, a donor, and suggest that the 2.330-eV line is an exciton bound to that donor, while the red emission is associated with a "donorlike center." All the evidence (lifetime, structure, field, and stress splittings) prove that the red center is an excitonic transition and the large binding energy of the exciton makes it highly unlikely that it is bound to an ionized donor or acceptor.³³ The annealing effect has also been observed in this laboratory; the intensity of the red center was always strongest after annealing in 1 atm of zinc vapor at 1000°C followed by rapid quenching. Furthermore, this effect is reversible, since slow cooling of an annealed crystal reduced the intensity of the red-center emission. It is felt that the oxygen is tied up with some other defect in the as-grown (or slowly cooled) crystal, forming a nonradiative complex. Annealing followed by quenching could dissociate this complex, leaving the oxygen in an isolated substitutional position. Possibly the line at 2.330 eV observed by Tanimizu and Otomo originates from the other member of this complex after dissociation.

ACKNOWLEDGMENTS

The author has benefitted from numerous discussions with J. J. Hopfield, D. G. Thomas, and R. A. Faulkner. Clarifying comments on the isotope shift have also been contributed by D. E. McCumber and R. E. Dietz. All the crystals for these experiments were grown by E. A. Sadowski, who also assisted with the optical experiments. The ZnO¹⁸ was prepared by R. B. Zetterstrom and the ZnTe source material was synthesized by R. T. Lynch. The argon-ion laser tube was supplied by E. I. Gordon. I would also like to thank P. J. Dean for critical reading of the manuscript.

³² S. Tanimizu and Y. Otomo, Phys. Letters **25A**, 744 (1967); **25A**, 745 (1967).

³³ J. J. Hopfield, *Proceedings of the International Conference on the Physics of Semiconductors, Paris, 1964*. (Academic Press Inc., New York, 1965), p. 725.